

# Phenotype of SARS-CoV-2-specific T-cells in COVID-19 patients with acute respiratory distress syndrome

*Daniela Weiskopf<sup>f1#</sup>, Katharina S. Schmitz<sup>2#</sup>, Matthijs P. Raadsen<sup>2</sup>, Alba Grifoni<sup>1</sup>, Nisreen M.A. Okba<sup>2</sup>, Henrik Endeman<sup>3</sup>, Johannes P.C. van den Akker<sup>3</sup>, Richard Molenkamp<sup>2</sup>, Marion P.G. Koopmans<sup>2</sup>, Eric C.M. van Gorp<sup>2</sup>, Bart L. Haagmans<sup>2</sup>, Rik L. de Swart<sup>2</sup>, Alessandro Sette<sup>1,4,5§</sup> & Rory D. de Vries<sup>2§\*</sup>*

<sup>1</sup> Center for Infectious Disease, La Jolla Institute for Immunology, La Jolla, CA92037, USA

<sup>2</sup> Department of Viroscience, Erasmus MC, Rotterdam, the Netherlands

<sup>3</sup> Department of Intensive Care, Erasmus MC, Rotterdam, the Netherlands

<sup>4</sup> Department of Pathology, University of California, San Diego, CA92037, USA

<sup>5</sup> Department of Medicine, University of California, San Diego, CA92037, USA

# equal first author contribution

§ equal last author contribution

\* author for correspondence: [r.d.devries@erasmusmc.nl](mailto:r.d.devries@erasmusmc.nl)

## Abstract

COVID-19 is associated with lymphopenia and ‘cytokine storm’, but no information is available on specific cellular immune responses to SARS-CoV-2. Here, we characterized SARS-CoV-2-specific CD4<sup>+</sup> and CD8<sup>+</sup> T-cells in patients with acute respiratory distress syndrome. The spike protein (S) proved a potent T-cell antigen and specific T-cells predominantly produced Th1 cytokines. These novel data are important in vaccine design and will facilitate evaluation of vaccine candidate immunogenicity.

NOTE: This preprint reports new research that has not been certified by peer review and should not be used to guide clinical practice.

## Introduction

A novel coronavirus, named SARS-CoV-2, has been identified as the causative agent of a global outbreak of respiratory tract disease (COVID-19)<sup>1,2</sup>. On April 9<sup>th</sup>, over 1.5 million cases and more than 90,000 deaths were reported globally. COVID-19 is characterized by fever, cough, dyspnea and myalgia<sup>2</sup>, but in some patients the infection results in moderate to severe acute respiratory distress syndrome (ARDS), requiring invasive mechanical ventilation for a period of several weeks. COVID-19 patients may present with lymphopenia<sup>2,3</sup>, but the disease has also been associated with immune hyperresponsiveness referred to as 'cytokine storm'<sup>4</sup>. A transient increase in co-expression of CD38 and HLA-DR by T-cells, a phenotype of CD8<sup>+</sup> T-cell activation in response to viral infection, was observed concomitantly<sup>5</sup>. This increase in both CD4<sup>+</sup> and CD8<sup>+</sup> CD38<sup>+</sup>HLA-DR<sup>+</sup> T-cells preceded resolution of clinical symptoms in a non-severe, recovered, COVID-19 patient<sup>6</sup>.

Despite the large numbers of cases and deaths, no information is available on the phenotype of SARS-CoV-2-specific T-cells. Here, we stimulated peripheral blood mononuclear cells (PBMC) from eight COVID-19 patients with ARDS, collected up to three weeks after admission to the intensive care unit (ICU), with MegaPools (MP) of overlapping or prediction-based peptides covering the SARS-CoV-2 proteome<sup>7</sup>. We detected SARS-CoV-2-specific CD4<sup>+</sup> and CD8<sup>+</sup> T-cells in all COVID-19 patients, whereas peptide stimulation of healthy control PBMC samples collected before the outbreak showed no response. SARS-CoV-2-specific T-cells predominantly produced Th1 cytokines, although Th2 cytokines were also detected.

## Results

We included eight COVID-19 patients with moderate to severe ARDS in this study (Figure 1a). Patients were between 49 and 72 years old (average  $59 \pm 7$  years) and of mixed gender (4 female, 4 male). All patients tested SARS-CoV-2 positive by RT-PCR and were ventilated during their stay at the ICU. At the time of writing, 3 patients were transferred out of the ICU, 1 patient was deceased, and 4 patients were still in follow-up. Patients were treated with lung protective ventilation using the higher PEEP/lower  $FiO_2$  table of the ARDSnet and restrictive volume resuscitation. They received antibiotics as a part of a treatment regime aimed at selective decontamination of the digestive tract. No antiviral or immunomodulatory drugs were used. All patients were at the ICU and included shortly after ICU admission; self-reported illness varied between 5 and 14 days before inclusion (Figure 1a)

Phenotyping analysis of PBMC collected 14 days post inclusion via flow cytometry indicated that COVID-19 patients presented with low percentages of  $CD3^+$  T-cells in peripheral blood, corresponding to the previously reported lymphopenia ( $8.4 \pm 3.6\%$  in COVID-19 vs  $44.0 \pm 7.6\%$  in healthy controls [HC],  $p < 0.0001$ , Figure 1b)<sup>2,3</sup>.

CD4:CD8 ratios were increased in COVID-19 patients when compared to HC ( $6.2 \pm 3.0$  in COVID-19 vs  $2.4 \pm 1.0$  in HC,  $p = 0.0037$ , Figure 1c). This may reflect migration of  $CD8^+$  T-cells to the respiratory tract.

PBMC were stimulated with three different peptide MPs: MP\_S, MP\_CD4\_R and two MP\_CD8 pools. MP\_S contained 221 overlapping peptides (15-mers overlapping by 10 amino acids) covering the entire surface glycoprotein (spike, S) and can stimulate both  $CD4^+$  and  $CD8^+$  T-cells. MP\_CD4\_R contained 246 HLA class II predicted

epitopes covering all viral proteins except S, specifically designed to activate CD4<sup>+</sup> T-cells. The two MP\_CD8 pools combined contained 628 HLA class I predicted epitopes covering all SARS-CoV-2 proteins, specifically designed to activate CD8<sup>+</sup> T-cells<sup>7</sup>. Stimulation of PBMC collected 14 days post inclusion with the different peptide pools led to consistent detection of both CD4<sup>+</sup> and CD8<sup>+</sup> SARS-CoV-2-specific T-cells in all COVID-19 patients (Figure 2a and b). Specific activation of CD4<sup>+</sup> and CD8<sup>+</sup> T-cells was measured via cell surface expression of CD69 and CD137; phenotyping of memory subsets was based on surface expression of CD45RA and CCR7 (Supplementary Figure 1a-j).

Stimulation of PBMC with MP\_S and MP\_CD4\_R led to detection and activation of SARS-CoV-2 specific CD4<sup>+</sup> T-cells (0.89% in COVID-19 vs 0.03% in HC,  $p=0.0005$  for MP\_S and 0.49% in COVID-19 vs 0.02% in HC,  $p=0.0033$  for MP\_CD4\_R, Figure 1d). Overall, the MP\_S peptide pool induced stronger responses than the MP\_CD4\_R peptide pool, indicating that the S surface glycoprotein is a strong inducer of CD4<sup>+</sup> T-cell responses. Phenotyping of CD4<sup>+</sup>CD69<sup>+</sup>CD137<sup>+</sup> activated T-cells identified the majority of these SARS-CoV-2-specific T-cells as central memory T-cells based on CD45RA and CCR7 expression ( $T^{CM}$ ).  $T^{CM}$  express homing receptors required for extravasation and migration to secondary lymphoid tissues, but also have high proliferative capacity with low dependence on co-stimulation<sup>8,9</sup>.

SARS-CoV-2-specific CD8<sup>+</sup> T-cells were activated by both the MP\_S and MP\_CD8 peptide pools (0.97% in COVID-19 vs 0.03% in HC,  $p=0.0002$  for MP\_S and 0.26% in COVID-19 vs 0.02% in HC,  $p=0.0002$  for MP\_CD8, Figure 1e), confirming that the S surface glycoprotein also induces CD8<sup>+</sup> T-cell responses. Phenotyping of

CD8<sup>+</sup>CD69<sup>+</sup>CD137<sup>+</sup> activated T-cells showed that these had a mixed phenotype.

The majority of virus-specific CD8<sup>+</sup> T-cells was identified as CCR7<sup>-</sup> effector memory (T<sup>EM</sup>) or terminally differentiated effector (T<sup>EMRA</sup>)<sup>9</sup>. Both these CD8<sup>+</sup> effector subsets are potent producers of IFN $\gamma$ , contain preformed perforin granules for immediate antigen-specific cytotoxicity and home efficiently to peripheral lymphoid tissues<sup>8</sup>.

As production of pro-inflammatory cytokines can be predictive of severe clinical outcome for other viral diseases<sup>10</sup>, we measured antigen-specific production of 13 cytokines in cell culture supernatants from PBMC stimulated with MP\_S (Figure 1f, IL-21 data not shown), MP\_CD4\_R and MP\_CD8 (data not shown). Activation of PBMC by the overlapping S peptide pool led to a strong significant production of the Th1 cytokines IFN $\gamma$ , TNF $\alpha$  and IL-2 in COVID-19 patients when compared to HC. More characteristic Th2 cytokines (IL-5, IL-13, IL-9 and IL-10) were also consistently detected, albeit at low levels. IL-6 levels were not different between COVID-19 patients and HC, while IL-4 and IL-21 could not be detected at all. Antigen-specific production of cytokines related to a Th17 response was mixed; IL-17 production was not different between patients and HC, whereas IL-22 could be detected. Thus, stimulation of PBMC from COVID-19 patients with MP led to a balanced production of IFN $\gamma$ , TNF $\alpha$ , IL-2, IL-5, IL-13, IL-9, IL-10 and IL-22.

Finally, we studied the kinetics of development of virus-specific humoral and cellular immunity in the COVID-19 patients. Real time RT-PCR detection of SARS-CoV-2 genomes in respiratory tract samples showed a decreasing trend over time (Figure 2d, ANOVA repeated measures  $p < 0.001$ ) whereas virus-specific serum IgG antibody levels, measured by ELISA, showed a significant increase (Fig 2e, ANOVA repeated

measures,  $p < 0.001$ ). PBMC collected 0, 7, 14 or 21 days post inclusion (day 21 only available for two patients) were stimulated with MP\_S and activation of CD4<sup>+</sup> T-cells was again measured by expression of activation-induced cell surface markers. SARS-CoV-2-specific CD4<sup>+</sup> T-cells were detected in all patients, and frequencies of virus-specific responder cells increased significantly over time (ANOVA repeated measures,  $p < 0.001$ ).

## Discussion

Collectively, these data provide information on the breadth, kinetics and phenotype of virus-specific cellular immune responses in COVID-19 ARDS patients. We provide evidence that SARS-CoV-2-specific CD4<sup>+</sup> and CD8<sup>+</sup> T-cells appear in blood of ARDS patients in the first two weeks post onset of symptoms, and their frequency increases over time. The phenotype of the antigen-specific cellular immune response is balanced; SARS-CoV-2-specific CD4<sup>+</sup> T-cells in blood were typically central memory, CD8<sup>+</sup> T-cells typically had a more effector phenotype. It is tempting to speculate that the CD8<sup>+</sup> cytotoxic T-cells are predominantly responsible for the production of IFN $\gamma$ , whereas virus-specific CD4<sup>+</sup> T-cells could be responsible for the production of typical Th1 and Th2 cytokines. Elevated levels of IL-6 in patient plasma have previously been correlated to respiratory failure in COVID-19 patients<sup>11</sup>. Here, we could not detect increased specific production of IL-6 in PBMC stimulated with peptide pools, suggesting that virus-specific T-cells are not to blame for the production of IL-6 and the concomitant 'cytokine storm', but that these are predominantly mediated by innate immune cells.

Novel SARS-CoV-2 vaccines are currently in development and mainly focus on the surface glycoprotein S as an antigen for efficient induction of virus-specific neutralizing antibodies. We now show that S can also be a potent immunogen for inducing virus-specific CD4<sup>+</sup> and CD8<sup>+</sup> T-cells, and our data combined with a previous study in a non-severe, recovered, COVID-19 patient<sup>6</sup>, indicate that virus-specific T-cells could be beneficial for a good clinical outcome. Collectively, these novel data are important for vaccine design and will facilitate the evaluation of future vaccine immunogenicity.

## **Acknowledgements**

We thank all health care workers and laboratory personnel who contributed to treatment and diagnosis of these and other COVID-19 patients. Specifically, we thank Jeroen van Kampen, Corine Geurts van Kessel, Annemiek van der Eijk and Marshall Lammers for their contributions to these studies.

## **Author contributions**

DW, AG, RLdS, AS and RDdV conceived and planned the experiments. DW, KSS, MPR, NMAO, RM and ECMvG contributed to sample preparation. DW, KSS, MPR, AG, NMAO, HE, JPCvsA, RM and RDdV carried out the experiments. DW, KSS, AG, MPGK, BLH, RLdS, AS and RDdV contributed to the interpretation of the results. RDdV took the lead in writing the manuscript, DW, KSS and RLdS contributed significantly. All authors provided critical feedback and helped shape the research, analysis and manuscript.

## **Competing interest statement**

The authors declare no competing interests.



## Figures

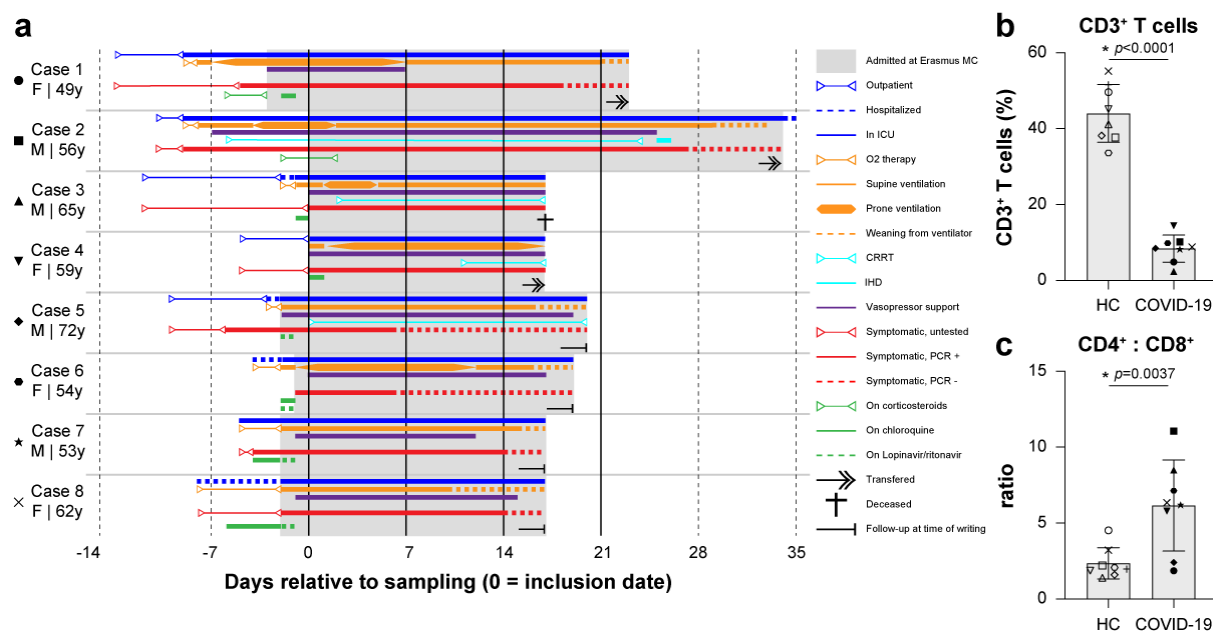


**Figure 1. Clinical overview of moderate to severe COVID-19 ARDS patients.** (a) Symptoms, hospitalization status, treatment and follow-up of COVID-19 ARDS patients included in this study. Patients were followed at the ICU up to 21 days post inclusion. Symbols shown next to the cases match throughout figures 1 and 2. (b) In PBMC collected 14 days post inclusion, percentages CD3<sup>+</sup> T-cells were significantly lower in COVID-19 patients compared to healthy controls (HC), while (c) CD4:CD8 ratios were increased. Panels b and c show individual values for n=8 patients versus n=8 HC, as well as the mean  $\pm$  SD. Asterisk denotes a significant difference.

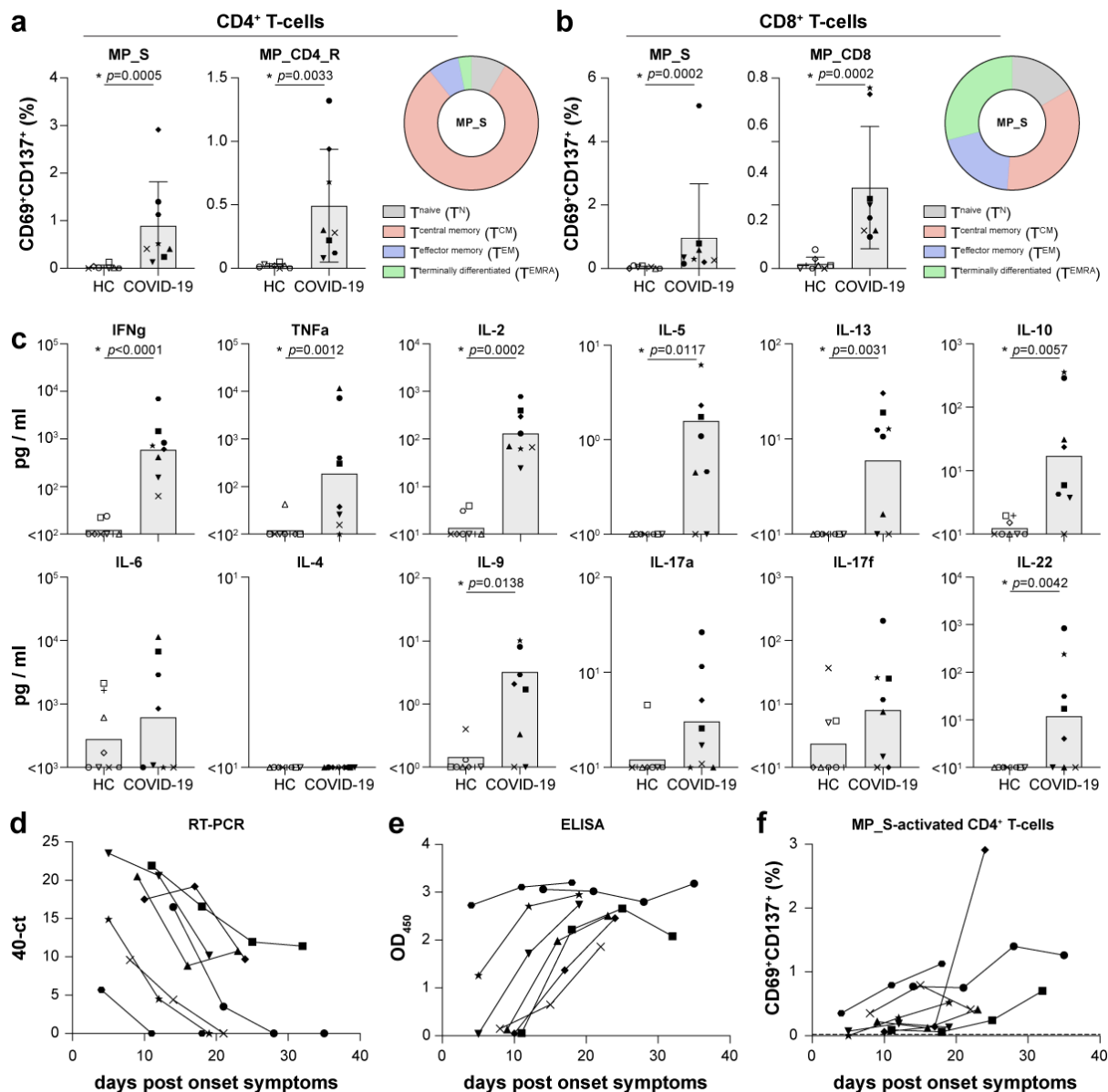


**Figure 2. Overview of SARS-CoV-2-specific immune response in COVID-19**

**ARDS patients.** (a and b) Antigen-specific activation of CD4<sup>+</sup> and CD8<sup>+</sup> T-cells in COVID-19 patients after stimulation with peptide MegaPools (MP), measured via cell surface expression of CD69 and CD137 (gating in supplementary figure 1). MP\_S induced the strongest activation. MP\_CD4\_R and MP\_CD8 also activated T-cells. Activated CD4<sup>+</sup> T-cells were phenotyped as predominantly central memory T-cells, whereas activated CD8<sup>+</sup> T-cells displayed a mixed memory phenotype (gating in

supplementary figure 1). (c) Antigen-specific production of cytokines measured in cell culture supernatants from PBMC stimulated with MP\_S. Activation by overlapping S peptides led to strong antigen-specific production of Th1 cytokines IFN $\gamma$ , TNF $\alpha$  and IL-2. Simultaneously, Th2 cytokines (e.g. IL-5, IL-13, IL-10 and IL-9) could be consistently detected. IL-4 was not detected, while IL-6 levels were not different between COVID-19 patients and HC. Th17 cytokines IL-17a and IL-17F were not significantly different between patients and HC, whereas IL-22 was produced. Bar charts in panels a, b and c show individual values for n=8 patients versus n=8 HC, as well as the mean  $\pm$  SD (SD is not shown for panel c). Asterisk denotes a significant difference ( $p < 0.05$ ). Sequential measurements of SARS-CoV-2 genomes detected in respiratory samples by realtime RT-PCR (40-ct, d), SARS-CoV-2-specific serum IgG antibody levels (OD<sub>450</sub>, e) and percentage SARS-CoV-2-specific CD4<sup>+</sup> T cells after MP\_S stimulation of PBMC (f), plotted against days post onset of symptoms. Genome levels showed a significant decrease over time, whereas antibody levels and specific T-cell frequencies significantly increased ( $p < 0.001$ , ANOVA repeated measures).

## Methods

**Ethical statement.** Patients admitted into the intensive care unit (ICU) with Acute Respiratory Distress Syndrome (ARDS) resulting from SARS-CoV-2 infection at Erasmus MC, Rotterdam, the Netherlands were included in a biorepository study aimed at ARDS and sepsis in the ICU. The first EDTA blood samples for PBMC isolation were obtained no more than 2 days after admission into the Erasmus MC ICU until 21 days post inclusion for as long as the patient was in the ICU. Patient care and research were conducted in compliance within guidelines of the Erasmus MC and the Declaration of Helsinki. Due to the clinical state of most ARDS patients (*i.e.* intubated, comatose), deferred proxy consent was obtained instead of direct written informed consent from the patients themselves. Retrospective written informed consent was obtained from patients after recovery. The study protocol was approved by the medical ethical committee of Erasmus MC, Rotterdam, the Netherlands (MEC-2017-417 and MEC-2020-0222). For experiments involving healthy control human buffy coats, written informed consent for research use was obtained by the Sanquin Blood Bank (Rotterdam, the Netherlands).

**Diagnosis.** Realtime RT-PCR on the E-gene was performed as described previously<sup>12</sup> on RNA isolated from sputa, nasopharyngeal or oropharyngeal swabs by MagnaPure (Roche diagnostics, The Netherlands) using the total nucleic acid (TNA) isolation kit.

**PBMC isolation.** PBMC were isolated from EDTA blood samples. Tubes were centrifuged at 200g for 15 min to separate cellular parts. Plasma-containing fraction

was collected, centrifuged at 1200g for 15 minutes, plasma was aliquoted and stored at -20°C. The cellular fraction was reconstituted with phosphate-buffered saline (PBS) and subjected to Ficoll density gradient centrifugation (500g, 30min). PBMC were washed and frozen in 90% fetal bovine serum (FBS) and 10% dimethyl sulfoxide (DMSO, Sigma Life science) at -135°C. Upon use, PBMC were thawed in IMDM (Lonza, Belgium) supplemented with 10% FBS, 100 IU of penicillin/ml, 100 µg of streptomycin/ml (Lonza, Belgium) and 2 mM L-glutamine (Lonza, Belgium) (I10F medium). PBMC were treated with 50 U/ml benzonase (Merck) for 30min at 37°C prior to use in stimulation assays.

**Epitope MegaPool (MP) design and preparation.** SARS-CoV-2 virus-specific CD4 and CD8 peptides were synthesized as crude material (A&A, San Diego, CA), resuspended in DMSO, pooled and sequentially lyophilized as previously reported<sup>13</sup>. SARS-CoV-2 epitopes were predicted using the protein sequences derived from the SARS-CoV-2 reference (GenBank: MN908947) and IEDB analysis-resource as previously described<sup>7,14</sup>. Specifically, CD4 SARS-CoV-2 epitope prediction was carried out using a previously described approach in Tepitool resource in IEDB<sup>15,16</sup> similarly to what was previously described<sup>7</sup>, but removing the resulting Spike glycoprotein epitopes from this prediction (CD4-R(remainder) MP, n=246). To investigate in depth Spike-specific CD4<sup>+</sup> T-cells, overlapping 15-mer by 10 amino acids have been synthesized and pooled separately (CD-4 S(spike) MP, n=221). CD8 SARS-CoV-2 epitope prediction was performed as previously reported, using the NetMHCpan4.0 algorithm for the top 12 more frequent HLA alleles in the population ( HLA-A\*01:01, HLA-A\*02:01, HLA-A\*03:01, HLA-A\*11:01, HLA-A\*23:01, HLA-A\*24:02, HLA-B\*07:02, HLA-B\*08:01, HLA-B\*35:01, HLA-B\*40:01, HLA-

B\*44:02, HLA-B\*44:03) and selecting the top 1 percentile predicted epitope per HLA allele<sup>7</sup>. The 628 predicted CD8 epitopes were split in two CD8 MPs containing 314 peptides each.

**SARS-CoV-2 RBD ELISA.** Serum or plasma samples were analyzed for the presence of SARS-CoV-2 specific antibody responses using a validated in-house SARS-CoV-2 receptor binding domain (RBD) IgG ELISA as previously described<sup>17</sup>. Briefly, ELISA plates were coated with recombinant SARS-CoV-2 RBD protein. Following blocking, samples were added and incubated for 1 hour, after which the plates were washed and a secondary HRP-labelled rabbit anti-human IgG (DAKO) was added. Following a 1 hour incubation, the plates were washed, the signal was developed using TMB, and the OD<sub>450</sub> was measured for each well.

**Ex vivo stimulations.** PBMC were plated in 96-wells U bottom plates at  $1 \times 10^6$  PBMC per well in RPMI1640 (Lonza, Belgium) supplemented with 10% human serum, 100 IU of penicillin/ml, 100 µg of streptomycin/ml (Lonza, Belgium) and 2 mM L-glutamine (Lonza, Belgium) (R10H medium) and subsequently stimulated with the described CD4 and CD8 SARS-CoV-2 MPs at 1µg/ml. A stimulation with an equimolar amount of DMSO was performed as negative control, phytohemagglutinin (PHA, Roche, 1µg/ml) and stimulation with a combined CD4 and CD8 cytomegalovirus MP (CMV, 1µg/ml) were included as positive controls. Twenty hours after stimulation cells were stained for detection of activation induced markers and subjected to flow cytometry. Supernatants were harvested for multiplex detection of cytokines.

**Flow cytometry.** Activation-induced markers were quantified via flow cytometry (FACSLyric, BD Biosciences). A surface staining on PBMC was performed with anti-CD3<sup>PerCP</sup> (BD, clone SK7), anti-CD4<sup>V450</sup> (BD, clone L200), anti-CD8<sup>FITC</sup> (DAKO, clone DK25), anti-CD45RA<sup>PE-Cy7</sup> (BD, clone L48), anti-CCR7<sup>APC</sup> (R&D Systems, clone 150503), anti-CD69<sup>APC-H7</sup> (BD, clone FN50) and anti-CD137<sup>PE</sup> (Miltenyi, clone 4B4-1). T-cell subsets were identified via the following gating strategy: LIVE CD3<sup>+</sup> were selected and divided in CD3<sup>+</sup>CD4<sup>+</sup> and CD3<sup>+</sup>CD8<sup>+</sup>. Within the CD4 and CD8 subsets, memory subsets were gated as CD45RA<sup>+</sup>CCR7<sup>+</sup> (naive, T<sup>n</sup>), CD45RA<sup>-</sup>, CCR7<sup>+</sup> (central memory, T<sup>CM</sup>), CD45RA<sup>-</sup>CCR7<sup>-</sup> (effector memory, T<sup>EM</sup>) or CD45RA<sup>+</sup>CCR7<sup>-</sup> (terminally differentiated effectors, T<sup>EMRA</sup>). T-cells specifically activated by SARS-CoV-2 were identified by upregulation of CD69 and CD137. An average of 500,000 cells was always acquired, the gating strategy is schematically represented in (Supplementary Figure 1A-J). In analysis, PBMC stimulated with MP\_CD8\_A and MP\_CD8\_B were concatenated and analyzed as a single file for SARS-CoV-2-specific responses to MP\_CD8.

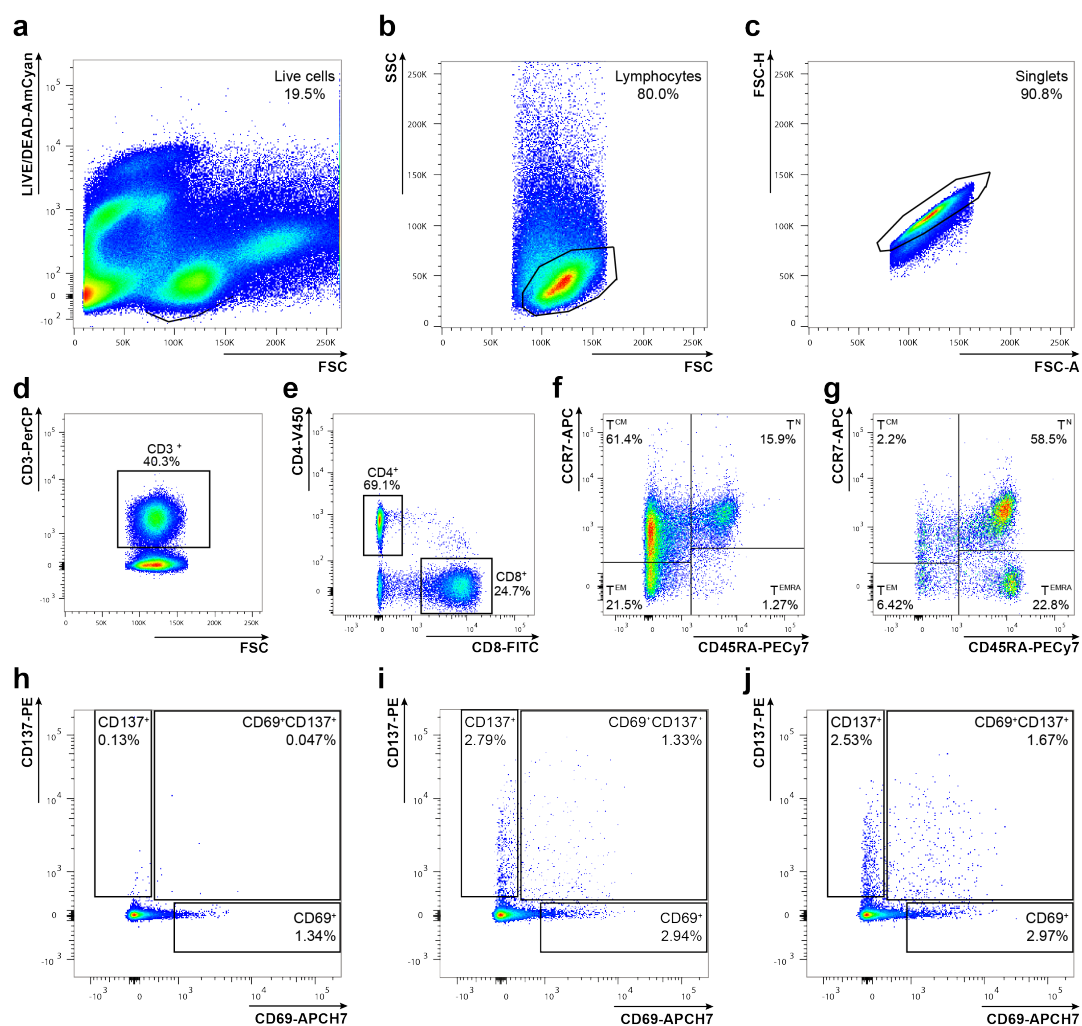
**Multiplex detection of cytokines.** Cytokines in cell culture supernatants from *ex vivo* stimulations were quantified using a human Th cytokine panel (13-plex) kit (LEGENDplex, Biolegend). Briefly, cell culture supernatants were mixed with beads coated with capture antibodies specific for IL-5, IL-13, IL-2, IL-6, IL-9, IL-10, IFN $\gamma$ , TNF $\alpha$ , IL-17a, IL-17F, IL-4, IL-21 and IL-22 and incubated for 2 hours. Beads were washed and incubated with biotin-labelled detection antibodies for 1 hour, followed by a final incubation with streptavidin<sup>PE</sup>. Beads were analyzed by flow cytometry. Analysis was performed using the LEGENDplex analysis software v8.0, which distinguishes between the 13 different analytes on basis of bead size and internal

dye. Quantity of each respective cytokine is calculated on basis of intensity of the streptavidin<sup>PE</sup> signal and a freshly prepared standard curve.

**Statistical analysis.** For comparison of CD3<sup>+</sup> T-cell percentages, CD4:CD8 ratios, CD69<sup>+</sup>CD137<sup>+</sup> stimulated T-cells and cytokine levels between HC and COVID-19 patients all log transformed data was tested for normal distribution. If distributed normally, groups were compared via an unpaired T test. If not distributed normally, groups were compared via a Mann-Whitney test. Two-tailed *p* values are reported throughout the manuscript. One way ANOVA repeated measures was used to test for linear trend over sequential time points (0, 7 and 14 days post inclusion).



## Supplementary Figure



**Supplemental figure 1.** (a-j) Gating strategy for detection of antigen-specific T cells after stimulation of PBMC. (a) Live cells were selected, (b) followed by the selection of lymphocytes and (c) singlets. (d) CD3<sup>+</sup> T cells were gated and (e) divided into CD4<sup>+</sup> and CD8<sup>+</sup> T cells. Both subsets were phenotyped as naïve (T<sup>N</sup>), central memory (T<sup>CM</sup>), effector memory (T<sup>EM</sup>) or terminally differentiated effectors (T<sup>EMRA</sup>) via measuring expression of CD45RA and CCR7 (f for CD4<sup>+</sup> T cells, g for CD8<sup>+</sup> T cells). (h-j) Within the different subsets, activated cells were identified via surface upregulation of activation induced markers CD69 and CD137. Percentages of CD69<sup>+</sup>CD137<sup>+</sup> double positive cells, reflecting activated cells, were used for further analysis. (h) DMSO (vehicle of the peptide pools) was included as a background

control, (i) CMV peptides or phytohemagglutinin were included as a positive control.

(j) Activation after stimulation could be observed in almost all PBMC samples from COVID-19 patients, whereas this activation was not observed in healthy controls (HC).

## References

1. Chan, J.F., *et al.* A familial cluster of pneumonia associated with the 2019 novel coronavirus indicating person-to-person transmission: a study of a family cluster. *Lancet* **395**, 514-523 (2020).
2. Huang, C., *et al.* Clinical features of patients infected with 2019 novel coronavirus in Wuhan, China. *Lancet* **395**, 497-506 (2020).
3. Chen, G., *et al.* Clinical and immunologic features in severe and moderate Coronavirus Disease 2019. *J Clin Invest* (2020).
4. Mehta, P., *et al.* COVID-19: consider cytokine storm syndromes and immunosuppression. *Lancet* **395**, 1033-1034 (2020).
5. Xu, Z., *et al.* Pathological findings of COVID-19 associated with acute respiratory distress syndrome. *Lancet Respir Med* **8**, 420-422 (2020).
6. Thevarajan, I., *et al.* Breadth of concomitant immune responses prior to patient recovery: a case report of non-severe COVID-19. *Nat Med* (2020).
7. Grifoni, A., *et al.* A Sequence Homology and Bioinformatic Approach Can Predict Candidate Targets for Immune Responses to SARS-CoV-2. *Cell Host Microbe* (2020).
8. Sallusto, F., Lenig, D., Forster, R., Lipp, M. & Lanzavecchia, A. Two subsets of memory T lymphocytes with distinct homing potentials and effector functions. *Nature* **401**, 708-712 (1999).
9. Mahnke, Y.D., Brodie, T.M., Sallusto, F., Roederer, M. & Lugli, E. The who's who of T-cell differentiation: human memory T-cell subsets. *Eur J Immunol* **43**, 2797-2809 (2013).

10. Wang, Z., *et al.* Early hypercytokinemia is associated with interferon-induced transmembrane protein-3 dysfunction and predictive of fatal H7N9 infection. *Proc Natl Acad Sci U S A* **111**, 769-774 (2014).
11. Herold, T., *et al.* Level of IL-6 predicts respiratory failure in hospitalized symptomatic COVID-19 patients. *MedRxiv* (2020).
12. Corman, V.M., *et al.* Detection of 2019 novel coronavirus (2019-nCoV) by real-time RT-PCR. *Euro Surveill* **25**(2020).
13. Carrasco Pro, S., *et al.* Automatic Generation of Validated Specific Epitope Sets. *J Immunol Res* **2015**, 763461 (2015).
14. Dhanda, S.K., *et al.* IEDB-AR: immune epitope database-analysis resource in 2019. *Nucleic Acids Res* **47**, W502-W506 (2019).
15. Paul, S., *et al.* Development and validation of a broad scheme for prediction of HLA class II restricted T cell epitopes. *J Immunol Methods* **422**, 28-34 (2015).
16. Paul, S., Sidney, J., Sette, A. & Peters, B. TepiTool: A Pipeline for Computational Prediction of T Cell Epitope Candidates. *Curr Protoc Immunol* **114**, 18 19 11-18 19 24 (2016).
17. Okba, N.M.A., *et al.* Severe Acute Respiratory Syndrome Coronavirus 2-Specific Antibody Responses in Coronavirus Disease 2019 Patients. *Emerg Infect Dis* **26**(2020).